ENTRANCE CHANNEL EFFECTS IN THE PRODUCTION OF EVAPORATION RESIDUES IN HEAVY ION FUSION REACTIONS

R.N.Sagaidak, G.N. Kniajeva, I.M. Itkis, M.G. Itkis, N.A. Kondratiev, E.M. Kozulin,

I.V. Pokrovsky, V.M. Voskressensky, A.V. Yeremin,

Flerov Laboratory of Nuclear Reactions, JINR, 141980 Dubna, Moscow region, Russia,

L. Corradi, A. Gadea, A. Latina, A.M. Stefanini, S. Szilner, M. Trotta, A.M. Vinodkumar,

INFN, Laboratori Nazionali di Legnaro, I-35020 Legnaro, Padova, Italy,

S. Beghini, G. Montagnoli, F. Scarlassara,

Dipartimento di Fisica and INFN, Università di Padova, I-35131 Padova, Italy

D. Ackermann,

GSI, D-64291 Darmstadt, and Johannes Gutenberg-Universität, D-55099 Mainz, Germany

N. Rowley,

IReS, UMR7500, IN2P3-CNRS/Université Louis Pasteur, F-67037 Strasbourg Cedex 2, France

Introduction and Motivation

In the framework of standard statistical model (SSM) approximations, information on fission barriers for heavy fissile nuclei can be extracted using experimental excitation functions for (HI, *xn*) reactions. Within the last thirty years a number of such attempts has been performed for different combinations of interacting nuclei using different approximations of SSM. The analysis performed in the framework of the potential barrier-passing model (BPM) for fusion and SSM incorporated into the HIVAP code [1] for nuclei ranging from Ra to U resulted in reduced values of the liquid-drop (LD) barriers. The obtained LD barriers were appreciably lower [2] than the ones obtained theoretically [3–5]. Some additional decrease in the LD-barriers for Th and U nuclei with neutron numbers close the N = 126 shell (corresponding to their relatively lower production cross sections) was assigned to the effect of the collective enhancement in the level density of the compound nucleus (CN) fission channel competing with evaporation channels leading to spherical nuclei [6]. It has to be noted that such effects are not taken into account in the HIVAP code.

At the same time, recent analysis of new data on the production of Th nuclei in the asymmetric ^{16}O + ^{204}Pb reaction [7] yields much higher values of the LD-barriers than ones obtained earlier [2], in the analysis of excitation functions for less asymmetric reactions as ^{40}Ar + $^{176\ldots180}$Hf [8]. It means that the fusion probability (or the CN formation probability) value adopted earlier as $P_{CN} = 1$ for the reactions induced by Ar and Ca ions [2], in fact, is much lower according to our new analysis of the data with the higher LD barriers, as is shown in **Fig.1** (see also Ref. [7] for details). Moreover, the recent data for the ^{216}Ra* CN formation in different combinations, reveal a marked suppression for the yield of Ra nuclei even in more asymmetric reactions induced by the ^{30}Si and even ^{19}F ions [9]. Following the results of our analysis [10] of the excitation functions for evaporation residues (ERs) and fission [9], this suppression corresponds to about 55% and 65% of the fusion probability for ^{30}Si and ^{19}F, respectively. Earlier, such fusion suppression was only observed in more symmetric reactions with massive partners [11–15] at incident energies around the nominal fusion barrier [16] and was explained by the quasi-fission (QF) effect. This is clearly manifested in the comparison of the ER cross sections for reactions leading to the same CN but differing in the entrance-channel mass-asymmetry [17]. Rather unexpectedly, QF is even manifested in rather asymmetric combinations with ^{19}F and ^{30}Si projectiles leading to the ^{216}Ra* CN [9].

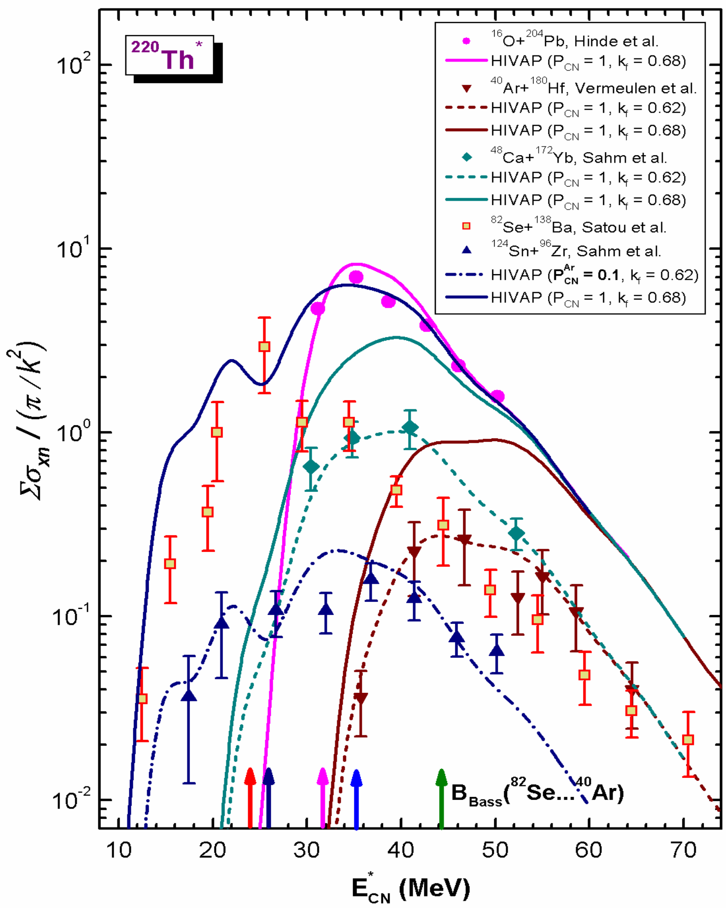

Fig. 1. Reduced cross sections for the production of Th nuclei in different reactions [8, 9, 12, 16] (symbols) in comparison with the HIVAP calculations [1] using different values of the scaling parameter at the LD fission barriers k_f and different values of the CN formation probability P_{CN} (lines).

In this report we present the results of measurements and analysis of the ER and fission excitation functions obtained in the very asymmetric ^{12}C + ^{204,206,208}Pb reactions leading to ^{216,218,220}Ra*, and in the more symmetric ^{48}Ca + ^{168,170}Er reactions leading to ^{216,218}Ra* [10]. The role of QF in the C + Pb reactions appears to be negligible, and so its excitation functions are a good reference point for applying the BPM coupled with SSM [1]. As the excitation functions for the production of Ra isotopes in the C + Pb reactions cover the region of neutron numbers 122 ≤ N ≤ 130, the effect of the N = 126 neutron shell could be studied. The results of the C + Pb analysis will then be applied to the study of ^{48}Ca + ^{168,170}Er. One should mention, that in our recent work on the comparative fission study in the ^{12}C + ^{204}Pb and ^{48}Ca + ^{168}Er reaction [18], a prominent QF component was observed in the mass and energy distributions of fission fragments for the more symmetric system.

A similar approach will be used in the analysis of the ^{48}Ca + ^{154}Sm reaction data [19] leading to the less fissile ^{202}Pb* CN, the same one obtained in the more asymmetric ^{16}O + ^{186}W reaction studied earlier [20]. Analysis of these data will be supplemented with the similar one for reactions leading to neighbor compound nuclei.

The study of effects of the entrance-channel mass-asymmetry, as well as of a different fissility of the CN formed in reactions, should help us to understand an influence of main reaction parameters on QF, i.e., on the fusion suppression in asymmetric reactions. This is important from the point of view of the analysis of reactions used for the synthesis of superheavy nuclei.

Experiment and Data Analysis

The experiments were carried out using ion beams from the XTU Tandem + ALPI accelerator complex of the Laboratori Nazionali di Legnaro. The beam intensity was monitored continuously using four silicon surface barrier detectors to measure Rutherford scattering from the target (below we shortly describe the experiments, see further details in Refs. [10, 18]).

Fission fragments were detected by the two-arm time-of-flight (TOF) spectrometer CORSET [18] installed inside the scattering chamber. The arms of the spectrometer were positioned so that the angle between the two detected fission fragments was $\theta_{c.m.} \approx 180°$. The data were analyzed event by event, the mass M and total kinetic energy TKE of the fragments being deduced from the measured velocities and positions. Binary events with full momentum transfer were selected using folding correlations corresponding to the double-differential cross sections $\partial^2\sigma/\partial M\partial TKE$ [18]. These differential cross sections were used to deduce total fission cross sections integrated both in and out of the reaction plane. This angular integration was performed for the symmetric-mass component [18] with an angular distribution given by the statistical transition-state model [21] for both the ^{12}C and ^{48}Ca induced reactions. The results are considered to give the CN-fission cross section. As an alternative approach, we also performed the angle integration over all fission-fragment masses between the light and heavy quasi-elastic peaks in the case of the ^{48}Ca reactions [18] (assuming a fission-fragment angular distribution $W(\theta_{c.m}) \sim 1/sin(\theta_{c.m})$) to estimate the total capture-fission cross sections (see, e.g., Ref. [22]).

Evaporation residues recoiling from the target were separated from the intense flux of beam-like particles using an electrostatic deflector (ED) [23]. The ED was set at $\theta_{lab} = 3^\circ$ to the beam direction for the ^{12}C reactions and at $\theta_{lab} = 1^\circ$ for the ^{48}Ca reactions in order to reduce the background of multiply scattered beam particles. For the ^{48}Ca reactions, the separated ERs passed through the start-detector of the TOF system and were implanted into a silicon surface-barrier stop-detector (SSBD) installed about 50 cm downstream. The resolution of this system allowed us to distinguish ERs unambiguously in the E–TOF spectra. For the ^{12}C reactions, the energy resolution of the SSBD for 5–10 MeV α-particles, allowed us to identify various $^{216,218,220}Ra^*$ evaporation channels from their known α-energies and those of their daughter products. The ER differential cross sections obtained at 3° and 1° were integrated using a gaussian fit to the measured angular distributions for $^{214,215}Ra$ produced in the $^{12}C + {}^{206}Pb$ reaction at E_{lab} = 73 MeV and for ERs detected in the $^{48}Ca + {}^{170}Er$ reaction at E_{lab} = 204 MeV. Angular distributions were measured by rotating the ED around the target position. The integrated cross sections were corrected for the ED transmission efficiency [23] using a Monte Carlo simulation developed for this purpose.

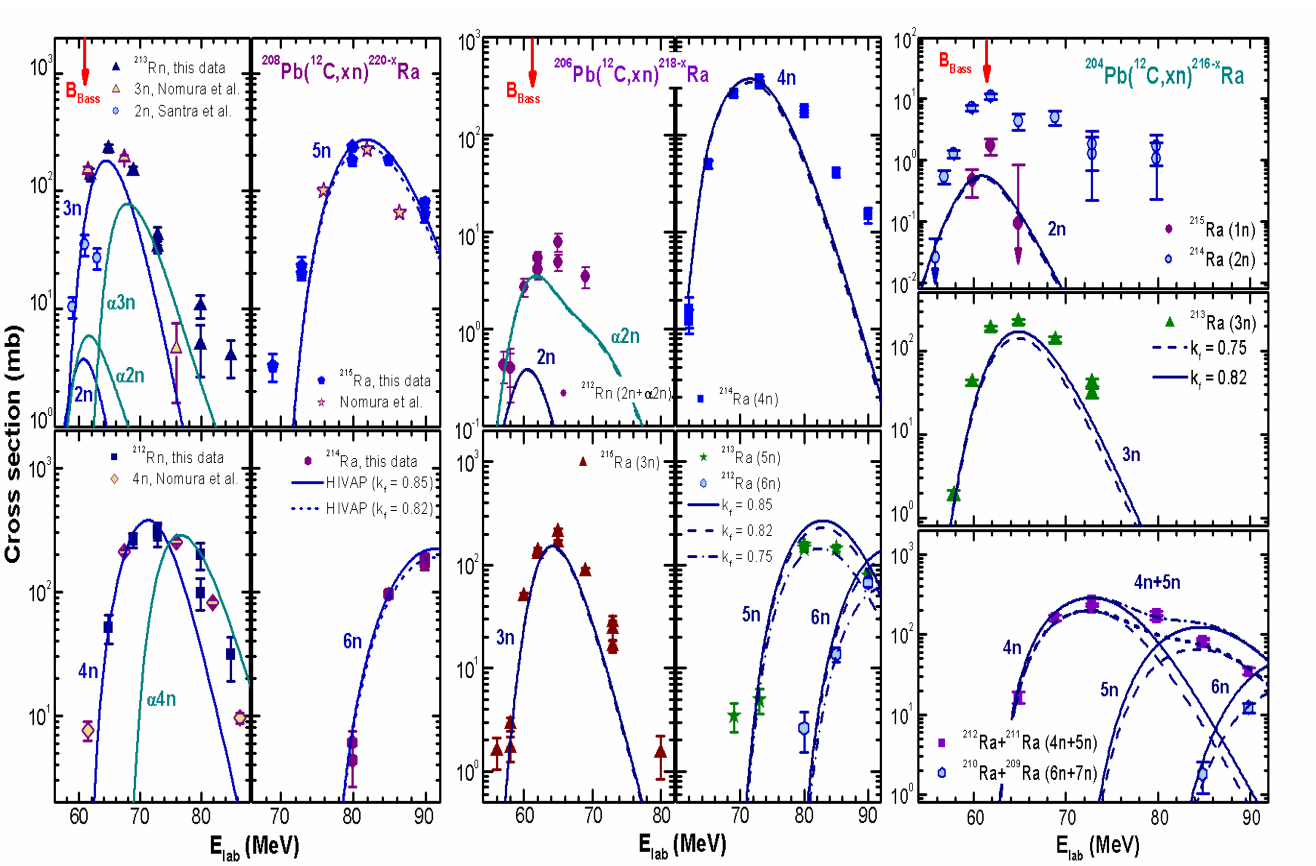

Fig. 2. Excitation functions for ERs obtained in our $^{12}C + {}^{204,206,208}Pb$ reactions study in comparison with the available data [24, 25] (symbols) and HIVAP calculations [1] using different k_f values (lines).

The ^{12}C + $^{204,206,208}Pb$ excitation functions for ERs observed in our study are shown in **Fig. 2** in comparison with the available data [24,25] and results of our calculations with HIVAP [1] using different values of the scaling parameter at the LD fission barriers k_f. One can see, that the production of the neutron-deficient Ra isotopes in the ^{12}C + ^{204}Pb reaction corresponds to a relative reduction in the LD fission barriers, as it follows from fit of calculated excitation functions to the data. The summarized picture of excitation functions for fission and ERs (a sum of the observed *xn* evaporation channels) is shown in **Fig. 3** together with other data, our calculations [10], and extracted values of the LD fission barriers for Ra nuclei.

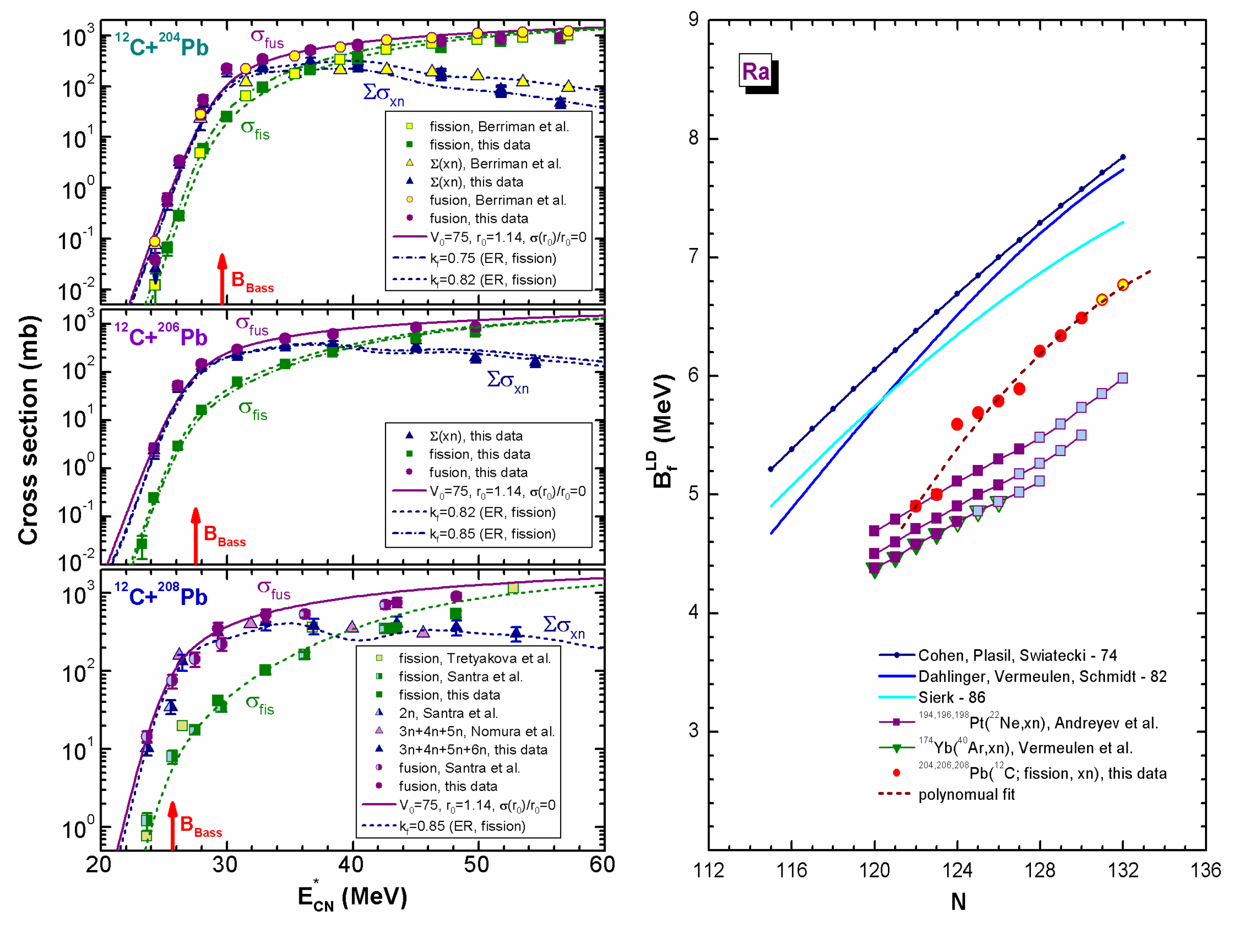

Fig. 3. Left panels — measured excitation functions (symbols) for ERs (sum of the *xn*-channels), fission and fusion obtained in the ^{12}C + $^{204,206,208}Pb$ reactions in comparison with the excitation functions calculated with HIVAP [1] (lines marked by $\boldsymbol{\Sigma\sigma_{xn}}$, $\boldsymbol{\sigma_{fis}}$ and $\boldsymbol{\sigma_{fus}}$), together with the values of the main parameters corresponding to the best fit to the data [10]. **Right panel** — extracted values of the LD fission barriers for Ra nuclei in comparison with results of the previous analysis [2] and calculated LD barriers [3–5].

The values of the LD fission barriers (k_f-values) were used in our analysis of the less asymmetric ^{22}Ne + $^{194,196,198}Pt$ systems studied earlier [26] and of the more symmetric ^{48}Ca + $^{168,170}Er$ systems studied in our experiments [10] as shown in **Fig. 4**. In the left panels of this figure, we compare the reduced ER cross sections (i.e., $(k^2/\pi)\cdot\Sigma\sigma_{xn}$, where k is the wave number) for the ^{12}C + $^{204,206,208}Pb$ and ^{22}Ne + $^{194,196,198}Pt$ reactions (leading to the same $^{216,218,220}Ra^*$ compound nuclei). As we have seen in the left panels, our calculations reproduce the C + Pb data and converge with similar calculations for Ne + Pt at energies well above the fusion barrier, where both reactions exhaust the angular momenta which may lead to evaporation. The experimental ER data do not converge, but show systematic differences between each pair of reactions, similar to the picture observed for reactions leading to $^{216}Ra^*$ [9] and $^{220}Th^*$ [7] (**Fig. 1**). Suppression factors for the ^{22}Ne induced reactions (or the fusion probability P_{fus} in our notation) are estimated to be about 40%. In the right panels, we present the results of our analysis of the more symmetric ^{48}Ca + ^{168,170}Er combinations. Again, using the same LD-fission barriers extracted from the C + Pb data analysis we underestimate the fission cross sections at sub-barrier energies and strongly overestimate the ER cross sections at all energies (short-dashed lines in the right panels in **Fig. 4**). This can be explained by the effect of QF inhibiting the fusion process, and we again introduce fusion probabilities to reproduce the data. Their values, derived from the ratio of the calculated ER cross sections to the measured ones (thick gray lines in **Fig. 4**), are within 0.31–0.35. The angle integration over all fission-fragment masses (see above) gives us an estimate of the total capture-fission cross sections. In this approach, considering the results as the total barrier-passing (capture) cross section, we obtain P_{fus} = 0.23–0.30. These values are lower than those obtained for the more asymmetric ^{19}F + ^{197}Au and ^{30}Si + ^{186}W systems [9].

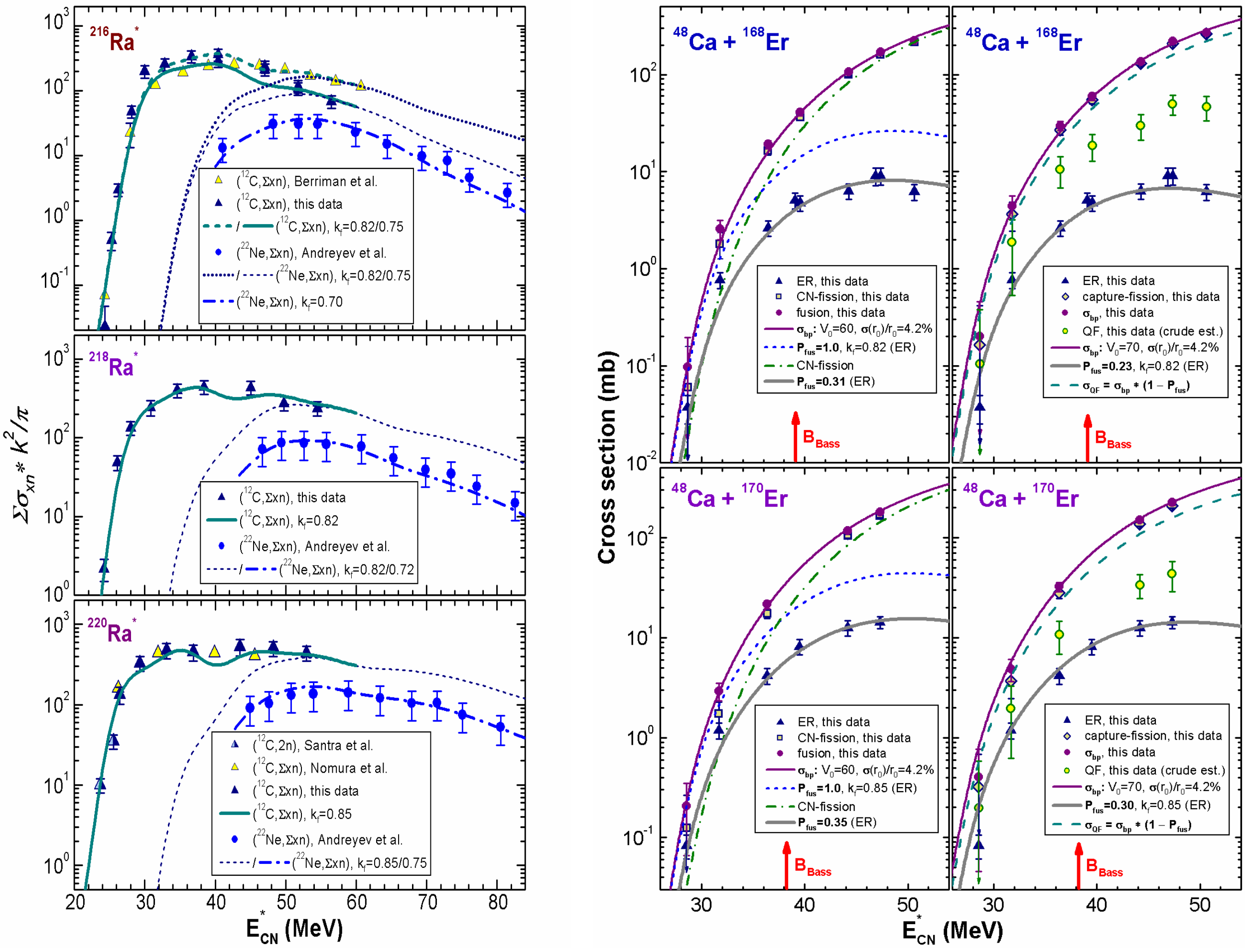

Fig. 4. The application of the LD fission barriers obtained in the C + Pb study to less asymmetric systems. **Left panels** — reduced cross sections for the production of Ra nuclei in the ^{12}C + ^{204,206,208}Pb and ^{22}Ne + ^{194,196,198}Pt (systematic errors corresponding to 40% cross section values have been added to the data [26]) reactions (symbols) in comparison with results of our calculations with HIVAP [1] including previous fit to the Ne + Pt data [2] (lines). **Right panels** — measured excitation functions for ERs (sum of all evaporation channels), CN-fission (capture-fission), fusion (barrier passing) and QF (crude estimates obtained as a difference between barrier passing and fusion cross sections) obtained in the ^{48}Ca + ^{168,170}Er reactions (symbols) in comparison with the excitation functions calculated with HIVAP [1] (lines). The values of the main parameters corresponding to the best fit to the data and derived values of the fusion probability (P_{fus}) are also shown.

Before discussing the results of our data analysis, let us summarized the main features of the used model. As mentioned in the introduction, our analysis is performed in the framework of the PBP model and the SSM incorporated into the HIVAP code [1]. The calculated ER cross sections for strongly fissile CN at energies well above the fusion barrier [16] are relatively insensitive to the form of the nuclear potential [14, 17] and are determined mainly by the SSM parameters describing the deexcitation of CN. The Reisdorf formula for the macroscopic parameters of the nuclear level density [1] leads to a ratio of the macroscopic level densities in the fission and evaporation channels $\widetilde{a}_f / \widetilde{a}_v \geq 1$ due to the different nuclear shapes at the saddle point (fission) and equilibrium state (particle emission). Ground-state shell effects are taken into account with a damping constant of 18.5 MeV [1], and are neglected at the saddle point. Empirical masses [28] were used to calculate ground-state shell corrections (ΔW_{gs} is the difference between the empirical and LD-masses), as well as for excitation energies and separation energies. Our calculations at energies above the fusion barrier depend only on one adjustable parameter k_f, the scaling factor of the rotating LD fission barriers $B_f^{LD}(\ell)$ [3] given by $B_f(\ell) = k_f \cdot B_f^{LD}(\ell) - \Delta W_{gs}$.

Barrier-passing cross sections were calculated in the framework of the PBP model using the exponential nuclear potential with sharp radius corrections. The radius parameter $r_0 = 1.14$ fm for the C + Pb reactions and 1.12 fm for Ca + Er with a diffuseness $d = 0.75$ fm in both cases. For the strength parameter of the nuclear potential, the best fit to the fusion data ($\sigma_{fus} = \sigma_{ER} + \sigma_{fis}$) yields $V_0 = 75$ MeV/fm for the C + Pb reaction and $V_0 = 60$ MeV/fm for Ca + Er. The values $r_0 = 1.14$ fm and $V_0 = 75$ MeV/fm were also found for $^{16}O + ^{208}Pb$ (fusion of spherical nuclei) [29], whereas our analysis of the Ca + Er data gave us the same values ($r_0 = 1.12$ fm and $V_0 = 60$ MeV/fm) as those obtained for other systems involving deformed targets: $^{40}Ar + ^{165}Ho \ldots ^{181}Ta$ [8, 30] and $^{40}Ar + ^{148,154}Sm$ [31]. Barrier fluctuations, expressed through the radius-parameter ratio $\sigma(r_0)/r_0$, were generated with a Gaussian distribution of r_0 around its average value. The best fit to the C + Pb fusion cross sections corresponds to $\sigma(r_0)/r_0 = 0$, whereas for the Ca + Er data we obtained $\sigma(r_0)/r_0 = 4.2\%$. These r_0 fluctuations simulate couplings to various entrance channels (e.g., projectile/target deformation) [31] to a degree sufficient for the present analysis. Transmission coefficients were obtained using the WKB approximation.

Discussion

As we have seen in **Figs. 2** and **3**, a satisfactory fit to the ER and fission excitation functions for the $^{12}C + ^{204,206,208}Pb$ reactions allows us to extract k_f values unambiguously. These values decrease from 0.85 to 0.75 as the neutron number decreases from 130 to 122, i.e., cross sections fall more rapidly than would follow from calculations with a fixed value of k_f. The same tendency was found in the region from Rn to U with some additional reductions in the LD barriers around N = 126 for Th, Pa and U nuclei [2]. As already mentioned, the latter was assigned to a collective enhancement in the level density of the fission channel [6], which was effectively taken into account in the similar analysis of [2] through the value of k_f. So, the manifestation of the N = 126 shell, at least in the production of ^{214}Ra and its neighbors, is not distinctly observed in comparison with the production of more remote Ra nuclei. The analysis presented in **Figs. 2** and **3** implies that all partial waves passing through the potential barrier lead to fusion, i.e., $\sigma_{bp} = \sigma_{fus} \equiv \sigma_{CN}$ or $P_{fus} = 1$ for the C + Pb systems. This is not the case for more symmetric massive systems. As shown in radiochemical studies of reaction products from such systems [13] and in the analysis of ER production in asymmetric and nearly symmetric reactions leading to the same CN [2, 17], σ_{fus} corresponds to a fraction of σ_{bp} (or $\sigma_{capture}$), i.e., $P_{fus} < 1$. Moreover, a similar situation is observed even for more asymmetric systems, as shown in Ref. [9] and by the present data.

It was quite unexpected for us that QF is also manifested in the $^{48}Ca + ^{154}Sm$ reaction [19] leading to the less fissile $^{202}Pb^*$ CN, the same one produced in the very asymmetric $^{16}O + ^{186}W$ combination [20]. In our analysis, as shown in **Fig. 5** (left panels), fitting the calculated barrier passing cross sections to the fusion data (estimated as $\sigma_{fus} = \sigma_{ER} + \sigma_{fis}$) for the $^{48}Ca + ^{154}Sm$ reaction (with the use of the same fission barriers as obtained in our fit to the $^{16}O + ^{186}W$ reaction data), we have obtained a marked overestimate of the ER production cross sections measured at energies above the barrier and a significant underestimate of the CN fission cross sections measured at energies below the fusion barrier. The fusion probability value for the ^{48}Ca + ^{154}Sm reaction is estimated to be 64%. This value is about twice bigger than those obtained in the ^{48}Ca + ^{168,170}Er reactions leading to the more fissile Ra compound nuclei [10]. The analysis shows that QF is manifested more strongly by comparing the capture-fission cross sections (all fission events) measured at sub-barrier energies with the calculated CN-fission excitation function. Moreover, the symmetric mass component in fission spectra, which is associated with the CN-fission, entirely disappears at energies well below the nominal fusion barrier [16]. Attempting to learn the effects of the entrance-channel mass-asymmetry and fissility of the CN on QF, we included in our analysis the data on the production of ^{200}Pb* [20, 32] and ^{194}Hg* [31, 33] in different reactions. The values of the fissility parameter x for these relatively weakly fissile compound nuclei are very close (0.686, 0.692 and 0.701 for ^{194}Hg*, ^{202}Pb* and ^{200}Pb*, respectively). Note, that no indications on the entrance-channel effect have been observed earlier in comparative studies of reactions leading to hardly-fissile ^{164}Yb* and ^{170}Hf* compound nuclei [34] (x = 0.611 and 0.625, respectively). Let us remind that in our study of reactions leading to the more fissile ^{216,218,220}Ra* CN (x = 0.745–0.751), a strong effect of the entrance-channel mass-asymmetry on the fusion probability has been observed [10, 18], whereas we have not found any signatures of QF in our analysis of the ^{30}Si + ^{170}Er reaction, the most symmetric combination leading to ^{200}Pb* as can be seen in **Fig. 5** (right panels).

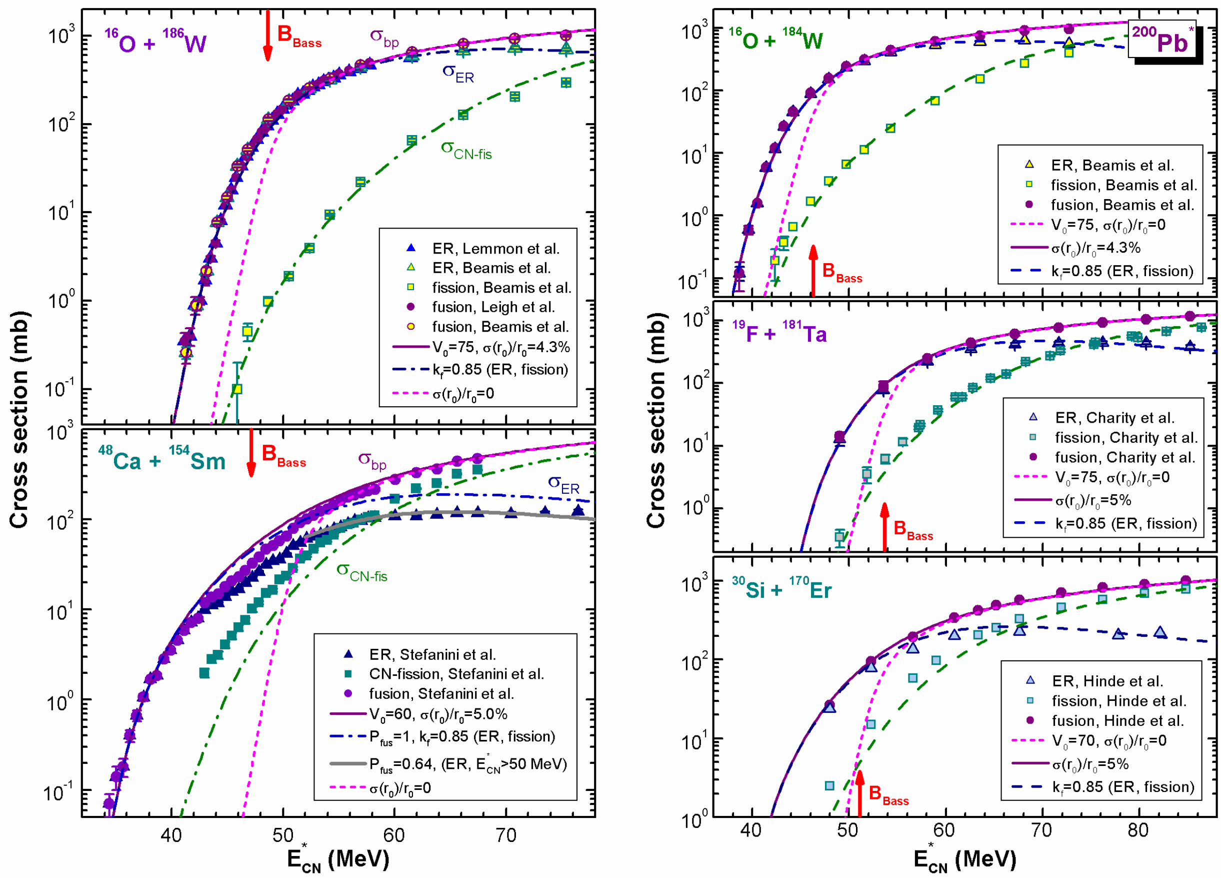

Fig. 5. The results of our analysis with HIVAP [1] (lines) of the ER, fission and fusion excitation functions measured in reactions with the different entrance-channel mass-asymmetry, which lead to formation of the ^{202}Pb* [19, 20] (**left panels**) and ^{200}Pb* [31, 32] (**right panels**) compound nuclei.

As we have seen, in contrast to the ^{202}Pb* data, all the excitation functions corresponding to the ^{200}Pb* CN formation are well reproduced in our calculations with close values of nuclear potential parameters and the same LD fission barriers (k_f value). So, one may conclude that no fusion suppression is observed for the production of CN with $x \approx 0.69$–0.70 in reactions with the entrance-channel mass-asymmetry $\alpha \geq 0.7$ [$\alpha = |A_p - A_t|/(A_p + A_t)$, where subscripts ($p$, t) refer to the projectile and target mass number, respectively], whereas a visible suppression is observed at $\alpha = 0.525$ in the ^{48}Ca + ^{154}Sm reaction.

In an attempt to find a threshold value for the entrance-channel mass-asymmetry corresponding to observable fusion suppression, we analyzed the data for the ^{40}Ar + ^{154}Sm reaction [31] (α = 0.588) together with available data for the very asymmetric ^{12}C + ^{182}W and ^{19}F + ^{175}Lu [33] combinations leading to the same ^{194}Hg* CN. The results show that fission data obtained in the ^{12}C + ^{182}W reaction at CN excitation energies E^*_{CN} < 80 MeV are fitted rather well with k_f = 0.92, whereas the similar ^{19}F + ^{175}Lu data are reproduced with the same value of the scaling parameter at E^*_{CN} > 80 MeV only. The value of k_f = 0.83 better fits lower excitation energies. The ER data at E^*_{CN} > 70 MeV lie somewhat between two excitation curves corresponding to these k_f values. So, the data for the very asymmetric reactions leading to ^{194}Hg* seem to lead to contradicting conclusions and have to be checked in independent experiments (for example, in the ^{16}O + ^{178}Hf reaction).

In **Fig. 6** (left panel), we present the fusion probability values obtained in our analysis of the data for systems with a different entrance-channel mass-asymmetry. Analyzed reactions lead to Yb, Hf, Pb, Ra, and Th compound nuclei having fissility parameter values spanning from 0.611 to 0.769 that corresponds to the region from hardly-fissile to strongly-fissile nuclei. As we have seen, the fusion probability values strongly decrease as the entrance-channel mass-asymmetry decreases for the reactions leading to strongly fissile compound nuclei. At the same time, the same tendency is appeared for weakly fissile nuclei and we do not observe any entrance channel effects in the reactions leading to hardly-fissile nuclei.

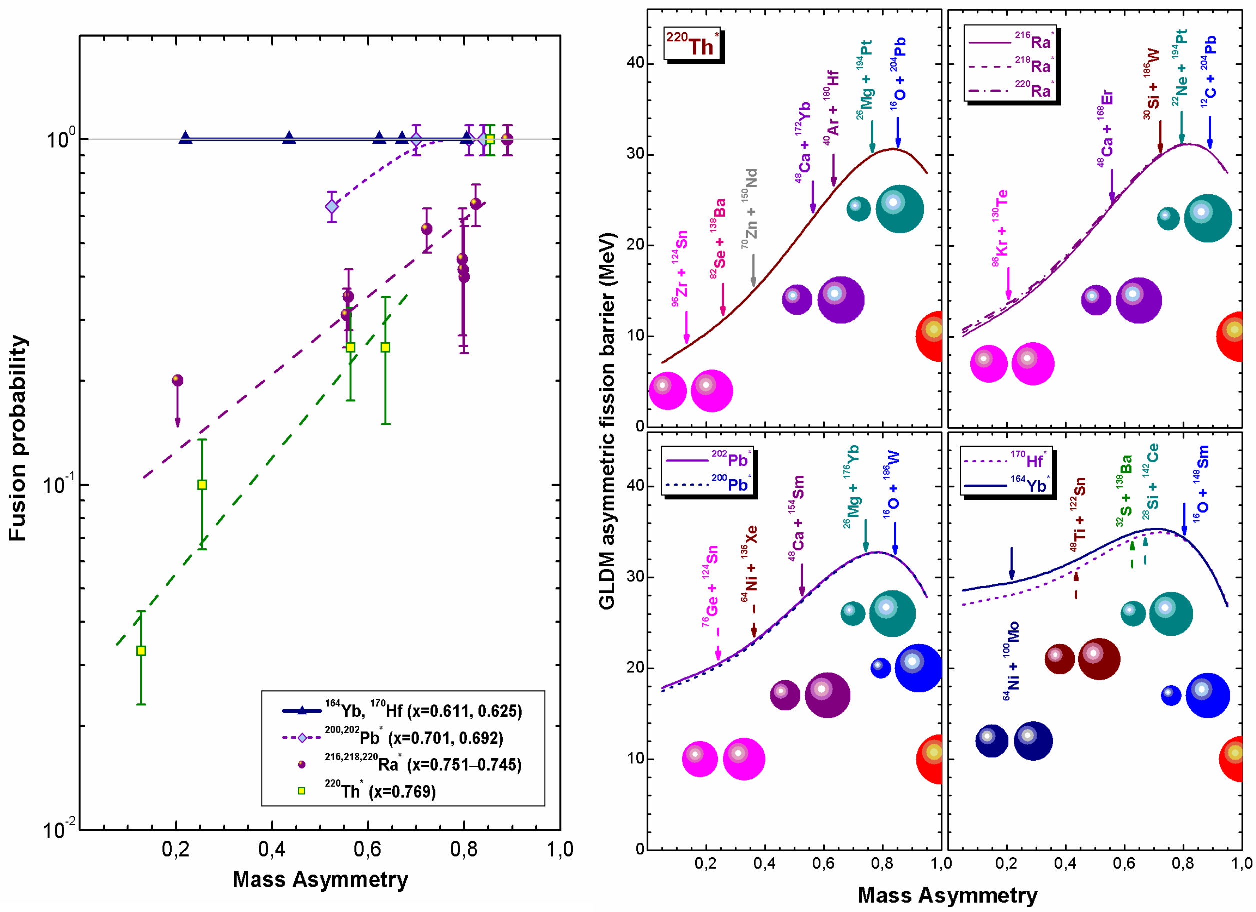

Fig. 6. Fusion probability values obtained in our analysis as a function of the entrance-channel mass-asymmetry for different systems leading to the same compound nuclei corresponding to different values of the fissility parameter (symbols) — **left panel** (lines are drawn to guide the eye). Asymmetric LD fission barriers obtained in the framework of the generalized LD model [35] for the systems considered in the present study as a function of the mass asymmetry parameter — **right panels** (arrows mark values of the asymmetry for some combinations analyzed in this work or could be studied in future and pairs of spheres sketch out configurations at the top of the barrier corresponding to the values of asymmetry marked by arrows).

Attempting to explain the observed effect of the mass-asymmetry on the fusion probability, we considered the asymmetric fission barriers obtained in the framework of the generalized LD model [35] as a function of the mass asymmetry parameter for the analyzed CN systems. As we have seen in **Fig. 6** (right panels), a value of the conditional barrier arising on the path along the mass-asymmetry coordinate to complete fusion leading to a spherical CN formation, anti-correlates (in general) with the fusion probability value, i.e., low fusion probability values ($P_{fus} \leq 0.3$) corresponding to relatively low mass asymmetry values ($\alpha \leq 0.6$) correlate with high conditional asymmetric-fission barrier values (greater than 5 MeV). At the same time, as we have seen, this approach is not sensitive to the changes in the potential energy less than 5 MeV, as we do not observe any correlations between the fusion probability values and an absence of any barrier for rather asymmetric combinations leading to fissile nuclei (at the top of the curves around the Businaro-Gallone point [36]). The same is related to the consideration of nearly symmetric combinations leading to hardly-fissile nuclei close to the region with A = 85–145 corresponding to the Businaro-Gallone plateau [36, 37]. One has to mention that in this qualitative approach we do not take into account shell corrections to the energy of nuclei. Accounting for them could significantly change the potential energy surface governing the evolution of two separate nuclei from their contact point to the compact form corresponding to their complete fusion.

Conclusion

In the conclusion, we underline that

- the collective enhancement in the nuclear level density is really manifested for Th nuclei produced in very asymmetric reactions in the vicinity of the N = 126 neutron shell, but not so strong as it was claimed earlier, in the study of less asymmetric combinations;

- the unexpected fusion suppression observed earlier for rather asymmetric combinations of colliding nuclei is really observed in other reactions with a close mass-asymmetry in the reaction entrance channel;

- the fusion probability value, as a measure of the fusion suppression, decreases with a decrease in the mass-asymmetry parameter value and with an increase in the CN fissility parameter.

Acknowledgements

The work was partially supported by the Russian Foundation for Basic Research (Grants Nos. 02-02-16-116, 99-02-17891) and by INTAS (Grant No. 00-655).

The Dubna team would like to thank INFN, Laboratori Nazionali di Legnaro for their warm hospitality and support of this work during its carrying out.

R.N.S. acknowledges the financial support from INFN during his stay in Legnaro.

References

1. W. Reisdorf, Z. Phys. A **300**, 227 (1981); W. Reisdorf and M. Schädel, Z. Phys. A **343**, 47 (1992).
2. R.N. Sagaidak *et al.*, in *Fusion Dynamics at the Extremes*, proceedings of the International Workshop, Dubna, 2000, edited by Yu.Ts. Oganessian and V.I. Zagrebayev (WS, Singapore, 2001) p. 135.
3. S. Cohen, F. Plasil, and W.J. Swiatecki, Ann. of Phys. **82**, 557 (1974).
4. M. Dahlinger, D. Vermeulen, and K.-H. Schmidt, Nucl. Phys. **A376**, 94 (1982).
5. A.J. Sierk, Phys. Rev. C **33**, 2039 (1986).
6. A.V. Ignatyuk *et al.*, Yad. Fiz. **37**, 831 (1983); A. B Junghans *et al.*, Nucl. Phys. **A629**, 635 (1998).

7. D.J. Hinde, M. Dasgupta, and A. Mukherjee, Phys. Rev. Lett. **89**, 282701 (2002).
8. D. Vermeulen *et al*., Z. Phys. A **318**, 157 (1984).
9. D.J. Hinde *et al*., J. Nucl. Radiochem. Sci. **3**, 31 (2002).
10. R.N. Sagaidak *et al*., Phys. Rev. C **68** (2003), in press.
11. C.-C. Sahm *et al.*, Nucl. Phys. **A441**, 316 (1985).
12. J. Töke *et al.*, Nucl. Phys. **A440**, 327 (1985); W.O. Shen *et al.*, Phys. Rev. C **36**, 115 (1987)
13. W. Reisdorf *et al.*, Z. Phys. A **342**, 411 (1992); P. Klein *et al.*, Z. Phys. A **357**, 193 (1997).
14. A.B. Quint *et al.*, Z. Phys. A **346**, 119 (1993).
15. K. Satou *et al.*, Phys. Rev. C **65**, 054602 (2002).
16. R. Bass, Phys. Rev. Lett. **39**, 265 (1977); Lect. Notes in Phys. **117**, 281 (1980).
17. R.N. Sagaidak *et al.*, in *Shells-50*, proceedings of the International Conference, Dubna, 1999, edited by Yu.Ts. Oganessian and R. Kalpakchieva (World Scientific, Singapore, 2000) p. 199.
18. A.Yu. Chizhov *et al.*, Phys. Rev. C **67**, 011603 (2003).
19. A.M. Stefanini *et al*., in *Nucleus-Nucleus Collisions 2003*, proceedings of the International Conference, Moscow, 2003, to be published.
20. C. E. Bemis, Jr. *et al*., ORNL Progress Report 1986 (ORNL-6326), p. 110; R.C. Lemmon *et al*., Phys. Lett. B **316**, 32 (1993); J.R. Leigh *et al*., Phys. Rev. C **52**, 3151 (1995).
21. R. Vandenbosch and J.R. Huizenga, *Nuclear Fission* (Academic, New York, 1973).
22. A.J. Pacheco *et al*., Phys. Rev. C **45**, 2861 (1992).
23. S. Beghini *et al*., Nucl. Inst. and Meth. in Phys. Res. A **239**, 585 (1985).
24. T. Nomura, K. Hiruta, T. Inamura, and M. Odera, Nucl. Phys. **A217**, 253 (1973).
25. S. Santra, P. Singh, S. Kailas, A. Shrivastava, and K. Mahata, Phys. Rev. C **64**, 024602 (2001).
26. A.N. Andreyev *et al*., Nucl. Phys. **A620**, 229 (1997).
27. W. Reisdorf *et al*., Nucl. Phys. **A444**, 154 (1985).
28. G. Audi and A.H. Wapstra, Nucl. Phys. **A595**, 509 (1995).
29. C.R. Morton *et al*., Phys. Rev. C **60**, 044608 (1999).
30. H.-G. Clerc *et al*., Nucl. Phys. **A419**, 571 (1984).
31. W. Reisdorf *et al*., Nucl. Phys. **A438**, 212 (1985).
32. D.J. Hinde *et al*., Nucl. Phys. **A385** 109 (1982); R.J. Charity *et al*., Nucl. Phys. **A457**, 441 (1986).
33. T. Sikkeland *et al*., Phys. Rev. C **3**, 329 (1971); S.K. Hui *et al*., Phys. Rev. C **62**, 54604 (2000).
34. N.G. Nicolis and D.G. Sarantites, Phys. Rev. C **48**, 2895 (1993); S. Gil *et al*., Phys. Rev. C **51**, 1336 (1995).
35. G. Royer and B. Remaud, Nucl. Phys. **A444**, 477 (1985); G. Royer, *et al.*, Nucl. Phys. **A634**, 267 (1998).
36. U. L. Businaro and S. Gallone, Nuovo Cim. **1**, 629, 1277 (1955).
37. L.G. Sobotka *et al*., Phys. Rev. Lett. **53** 2004 (1984).